References

[1] **Berberian, M., and King, G. C., 1981,** Towards a paleogeography and tectonic evolution of Iran: Canadian Journal of Earth Sciences, v. 18, p. 210-265.

[2] **Bodnar, R. J., 1992,** Experimental determination of the liquidus and isochores of a 40 wt % NaCl-H_2O solution using synthetic fluid inclusions [abs]: Pan-American Conf. Research Fluid Inclusions (PACROFI IV), Lake Arrowhead, CA, May 22-25, 1992 Program abstracts, v. 4, p. 14.

[3] **Chivas, A. R., and Wilkins, W. T., 1977,** Fluid inclusion studies in relation to hydrothermal alteration and mineralization at the Koloula porphyry copper prospect, Guadalcanal: ECONOMIC GEOLOGY, v. 72, p. 153-169.

[4] **Chou, I. M., 1987,** Phase relations in the system NaCl-KCl-H_2O. III: solubilities of halite in vapor-saturated liquids above 445 °C and redetermination of phase equilibrium properties in the system NaCl-H_2O to 1000 °C and 1500 bars, GEOCHIMICA ET COSMOCHIMICA ACTA. v. 51, p. 1965-1975.

[5] **Ghayori, 2000,** Petrographical studies on well No. 1, Report, Raigan samples, Bam.

[6] **Hezarkhani, A., 1997,** Physicochemical controls on alteration and copper mineralization in the Raigan porphyry copper system, Iran. Unpublished Ph.D thesis, Canada, University of McGill, 281 p.

[7] **Hezarkhani, A., 2002,** Specific Physico-Chemical Conditions (360 °C) for Chalcopyrite Dissolution/Deposition in the Sungun Porphyry Copper Deposit, Iran. AMIRKABIR JOURNAL OF SCIENCE AND TECHNOLOGY, v. 13, no. 52, p. 668-687.

[8] **Hezarkhani, A., (2003).** Mass Changes During the Hydrothermal Alteration/Mineralization in a Porphyry Copper Deposit, Eastern Sungun, Northwestern Iran, **Elsevier, Asian Earth Sciences,** (In press and appears at the following address).

[9] **Hezarkhani, A.,** Williams-Jones, A. E., and Gammons, C. H., (1999), Factors controlling copper solubility and chalcopyrite deposition in the Sungun porphyry copper deposit, Iran. Mineralium deposita, vol. 34, pp. 770-783.

[10] **Linke, W. F., 1965,** Solubilities of inorganic and metal organic compound, II, 4th ed. AMERICAN CHEMICAL SOCIETY, Washington, D. C.

[11] **Niazi, M., and Asoudeh, I., 1978,** The depth of seismicity in the kermanshah region of the Zagros mountains (Iran): EARTH AND PLANETARY SCIENCE LETTER, v. 40, p. 270-274.

[12] **Pourhosseini, F., 1981,** Petrogenesis of Iranian plutons: a study of the Natanz and Bazman intrusive complexes: Ph.D thesis, University of Cambridge, 315p.

[13] **Roedder, E., 1984,** Fluid inclusions: Reviews in mineralogy, Ribbe, P. H., ed., v. 12, 644p.

[14] **Stöcklin, J., 1977,** Structural correlation of the Alpine ranges between Iran and Central Asia. Mem. H. Aser. Soc. Geol. France, pp. 333-353.

[15] **Stöcklin, J., and Setudenia, A. 1972,** Lexique Stratigraphique International Volume III ASIE Centre National De La Recherche Scientifique. 15, quai Anole-France, pp. 75, (Paris-VII).

[16] **Shahabpour, J., 1994,** Post-mineralization breccia dike from the Sar Cheshmeh porphyry copper deposit, Kerman, Iran: Exploration and Mining geology, v. 3, p. 39-43.

[17] **Sterner, S. M., Hall, D. L., and Bodnar, R. J., 1988,** Synthetic fluid inclusions. V. Solubility of the system NaCl-KCl-H_2O under vapor-saturated conditions. GEOCHIMICA ET COSMOCHIMICA ACTA, v. 52, p. 989-1005.

[18] **Waterman, G. C., and Hamilton, R. L., 1975,** The Sar-Cheshmeh porphyry copper deposit, ECONOMIC GEOLOGY, v. 70, p. 568-576.

[19] **Werre, Jr., R. W., Bodnar, R. J., Bethke, P. M., and Barton, P. B., 1979,** A novel gas-flow fluid inclusion heating-freezing stage (abstr): GEOLOGICAL SOCIETY OF AMERICA. Abstract Programs, 11, p. 539.

Table (1) Fluid Inclusion Microthemometric Data From Raigan Area.

Sample[1]	Stage[2]	Origin[3]	Type[4]	Te (° C)		Tm_{ICE} (° C)		Tm_{Halite} (° C)		$Tm_{Sylvite}$ (° C)		Th_{L-V} (° C)		Salinity	
				range	Avg.	range	Avg.	range	Avg.	range	Avg.	range	Avg.	range	Avg
Rz-46	I	s	VL	-19.7 to -27.3 (5)	-24.7	-5.1 to -11.6 (5)	-7.7					350.0 to 420.0 (5)	382.0	13.5 to 10.8 (5)	12.2
Rz-46	I	ps	VL	-21.3 to -25.9 (7)	-23.1	-0.4 to 8.1 (7)	-4.1					587.1 to 598.0 (7)	590.5	11.2 to 1.1 (7)	6.1
Rz-46	III	ps	LV	-23.0 to -24.2 (3)	-22.1	-5.1 to -8.2 (3)	-6.3					523.0 to 298.1 (3)	400.2	8.9 to 11.7 (3)	5.7
Rz-63	I	ps	VL	-20.9 to -48.1 (3)	-38.2	-1.9 to -9.3 (3)	-6.1					600.0 to 428.0 (3)	500.3	2.1 to 18.3 (3)	12.2
Rz-63	I	p	$LVHS_2$	-47.0 to -64.0 (4)	-54.0	-8.3 to -23.7 (4)	-14.1	436.0 to 511.0 (4)	485.1	101.1 to 59.8 (4)	77	598.0 to 337.0 (4)	487.4	54.1 to 45.8 (4)	50.1
Rz-63	II	p	$LVHS_2$	-40.0 to -58.5 (5)	-53.6	-5.3 to -18.3 (5)	-13.5	523.0 to 375.0 (5)	443.2	94.5 to 64.9 (5)	80.6	556.0 to 578.0 (5)	543.4	61.7 to 42.1 (5)	52.8
Rz-63	II	ps	VL	-22.1 to -45.9 (3)	-37.6	-0.6 to -9.1 (3)	-5.3					397.4to 401.0 (3)	399.6	2.1 to 13.5 (3)	7.3
Rz-63	II	s	VL	-18.3 to -46.9 (6)	-30.8	-1.7 to -11.0 (6)	-8.9					347.0 to 600.0 (6)	429.2	1.9 to 15.0 (6)	9.1
Rz-116	I	p	$LVHS_1$	-57.1to -51 0 (4)	-53.3	-6.9.1 to -15.1 (4)	-10.1	502.0 to 447.2 (4)	487.8	120.0 to 91.1 (4)	102.3	521.0 to 510.0 (4)	515.8	60.5 to 48.7 (4)	61.2
Rz-116	II	ps	$LVHS_2$	-29.9 to -48.3 (4)	-40.2	-6.1 to -13.7 (4)	-8.9	490.0 to 421.2 (4)	456.3			400.0 to 340.0 (4)	357.0	55.1to 49.4 (4)	53.2
Rz-116	I	p	VL	-24.1 to -32.0 (3)	-27.3	-1.7 to -12.5 (3)	-6.9					>600	nd.	>17.8	nd.
Rz-87	I	p	$LVHS_1$	-38.3to -61.4 (4)	-49.1	-3.5 to -14.2 (4)	-9.2	432.0 to 520.0 (4)	461.3			353.1to 291.0 (4)	375.5	60.1 to 49.9 (4)	57.1
Rz-107	I	p	$LVHS_2$	-46.5 to -62.8 (3)	-53.9	-9.1 to -24.2 (3)	-13.9	552.0 to 519.0 (3)	532.1	109.1 to 76.8 (3)	82.6	589.0 to >600 (3)	598.4	62.1 to 55.8 (3)	61.1
Rz-49	I	ps	VL	-22.9 to -27.1 (5)	-24.5	-0.5 to -12.1 (5)	-3.9					455.4 to 351.5 (5)	387.3	14.9 to 1.4 (5)	6.3
Rz-49	I	p	$LVHS_2$	-46.9 to -64.2 (3)	-54.4	-98.1 to -24.0 (3)	-13.9	432.0 to 519.2 (3)	482.2	121.1 to 73.8 (3)	80.4	598.0 to 351.0 (3)	479.2	53.9 to 47.8 (3)	52.4
21.88	I	s	$LVHS_1$	-42.1 to -57.1 (4)	-51.2	-5.4 to -16.3 (4)	-15.5	537.0 to 381.3 (4)	451.2	91.2 to 63.2 (4)	79.1	549.0 to 576.1 (4)	560.4	61.1 to 47.3 (4)	54.1
21.90	I	s	$LVHS_1$	-39.8 to -54.3 (5)	-50.7	-6.7.4 to -17..1 (5)	-16.3	543.0 to 371.8 (5)	473.0	102.2 to 61.9 (5)	83.3	538.4 to 551.0 (5)	542.5	60.5 to 41.2 (5)	51.7

Number of inclusions measured is given in parenthesis.

[1] Numbers or sign before dash identify drill holes and those after the dash indicate the depth.

[2] Stage of mineralized quartz veins or rock samples (based on populations), [3] Fluid inclusion origin, P = primary, S = secondary, Ps = pseudosecondary, [4] Types of fluid inclusions.

Te = Eutectic temperature, Tm = ice melting temperature, Tm HH = ice melting temperature for hydrohylite, Th = homogenization temperature, Avg = average, nd=not defined.

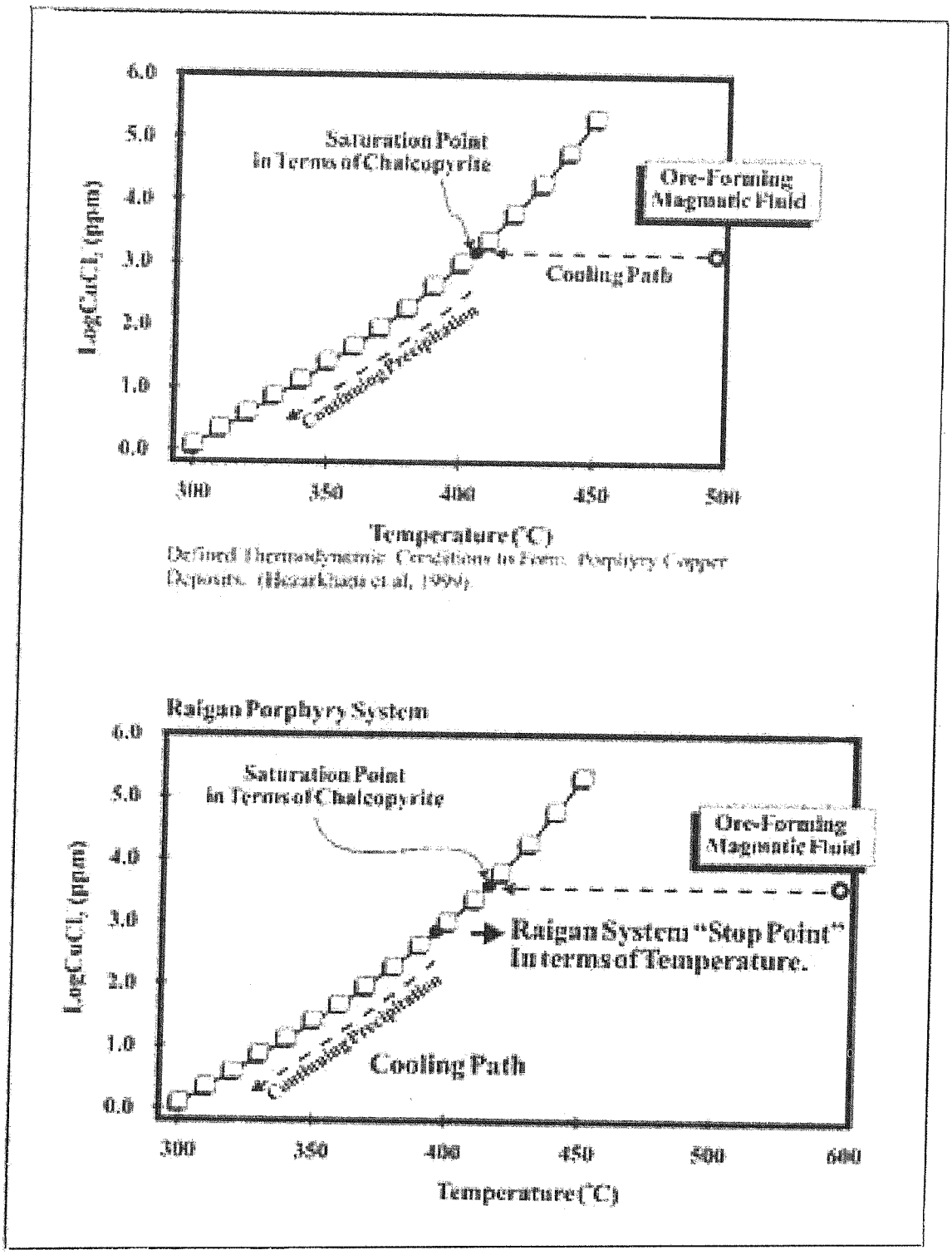

Figure (3) Solubility of chalcopyrite as a function of temperature at aCl^- = 1 m. Note that chalcopyrite solubility under the Raigan conditions is very strongly dependent on temperature, decreasing from >10,000 ppm at 600 °C, to about 1000 ppm at ~400 °C. Based on unknown reasons (need more investigations to identify them), system was not able to cool down continuously. It causes the system to keep copper chlorite complexes in the solution, instead of depositing it in the rock.

m) containing covellite, chalcocite and digenite, located below an intensely altered cap. Based on the present information, hydrothermal fluid in Raigan was too hot to be able to deposit the copper and continuation with re-concentration toward an economic porphyry tvpe deposit (Figure 3).

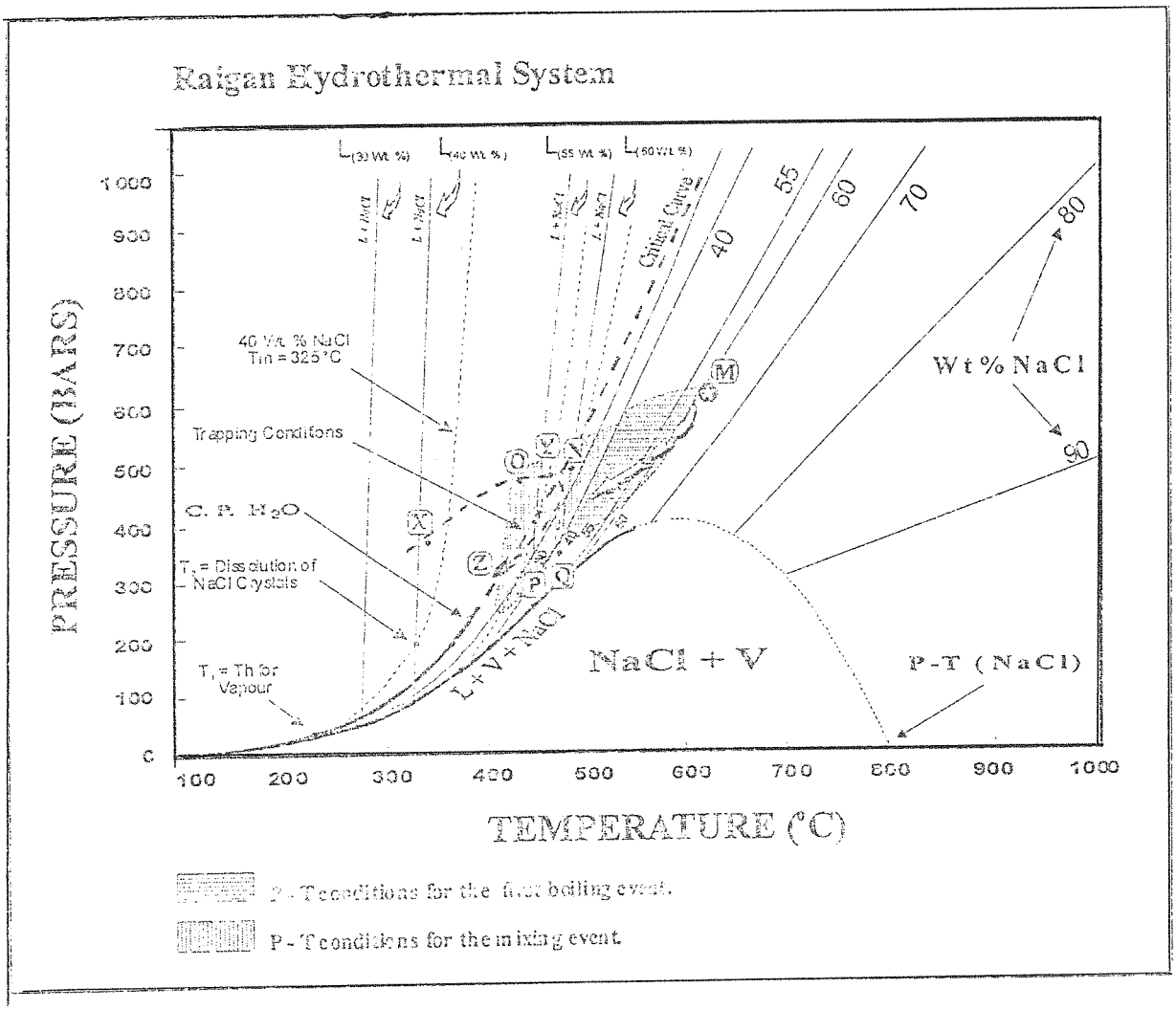

Figure (2) Pressure-temperature diagram for the system NaCl-H_2O showing the proposed mechanisms for the formation of the LVHS fluid inclusions VL and lower salinity LV inclusions. The LVHS inclusions are envisaged to represent part of a boiling fluid of orthomagmatic origin first trapped at a temperature of approximately 600 °C and pressure of 500 bars (M). M-N-O is the path that explains the $LVHS_1$ and $LVHS_2$ inclusions which homogenize by the halite disappearance. Liquids trapped between points N and O are in equilibrium with halite. To form the $LVHS_1$ fluid inclusions which homogenize by vapor disappearance, it is necessary to invoke sudden lowering of pressure along N-P or N-Q (isothermal) until the fluid is in equilibrium with vapor (see text for more information). Point X represents the assumed initial P-T conditions for the evolved meteoric fluid. This fluid moved downwards into the system and mixed with orthomagmatic fluids, thereby evolving along a path of increasing temperature and pressure. At point Y the fluid reached its maximum depth and subsequently ascended along an adiabatic cooling curve (Y-Z). Trapping of this fluid led to the formation of LV inclusions. Abbreviations: C.P.H_2O = critical point of water, L = Liquid, V = vapor, NaCl = halite. Diagram modified after Chou (1987), with liquidus curves from Bodnar (1992).

Fluid evolution

The high trapping temperatures and high salinity of $LVHS_1$ and $LVHS_2$ fluid inclusions suggest that Fluid population I and II probably represents an orthomagmatic fluid. We propose that this fluid exsolved as a high density phase from a diorite/granodiorite magma (the solidus temperature of this magma and emplacement pressure are above the critical point curve for high salinity fluids in the system NaCl-KCl-H_2O), and subsequently saturated with halite and boiled. Furthermore, it is proposed that the $LVHS_2$ fluid inclusions generally represent the pre-boiled fluid, and the $LVHS_1$ and VL inclusions, the high and low density products of boiling, respectively.

The interpretation that $LVHS_1$ fluid inclusions are the products of boiling is supported by the facts: 1) that they almost invariably homogenized by vapor disappearance; and 2) that they are commonly associated spatially with VL inclusions. We conclude that $LVHS_1$ and VL fluid inclusions record a later stage in the evolution of the Raigan hydrothermal system than the $LVHS_2$ fluid inclusions, i.e., a stage when conditions were closer to hydrostatic and Fluid I boiled extensively.

It is propose that the source of Fluid population II ($LVHS_2$ and VL fluid inclusions) was also mainly orthomagmatic (high salinity), but that this fluid circulated at lower temperature than Fluid I and mixed with an external fluid. This is also suggested by a weak trend from higher temperature and higher salinity to lower temperature and lower salinity in going from $LVHS_2$ to LV fluid inclusions. Coexistence of $LVHS_1$ fluid inclusions (which homogenize largely by vapor disappearance) with VL fluid inclusions indicate that Fluid II boiled extensively.

Fluid III (L-V inclusions) circulated mainly in veins at temperatures from 523.0 ° to 298.1 °C. It is proposed that the source of Fluid III was mainly meteoric water, and that it mixed to variable degrees with magmatic fluids. This conclusion is based on the decrease in salinity down to 5.7 wt % NaCl equiv. in LV fluid inclusions and the corresponding decrease in homogenization temperature.

Fluids II and I commonly occur in both quartz veins. It is interpreted this to record the downward movement of Fluid III (dominantly meteoric), which initially was at conditions indicated by point X on Figure 2, and its subsequent evolution along a path of increasing temperature due to mixing with orthomagmatic fluids, which originated at point M. At point Y the fluid reached its maximum depth and subsequently ascended along an adiabatic cooling curve (Y-Z).

Conclusions

The multiple intrusions of dioritic and granodioritic to quartz-monzonitic rocks at Raigan (Ghayori, 2000) indicate a long-lived intrusive episode associated with repeated fracturing and hydrothermal activity. Mineralogical and fluid inclusion analyzes from the system indicate three distinct hydrothermal fluids. The first hydrothermal fluid caused potassic alteration and very low Cu mineralization due to very high temperature conditions. This fluid was characterized by very high temperatures and high salinities, and was magmatically derived. It was responsible for the wide distribution of population I and II mineralized quartz veins and boiled episodically. The second hydrothermal fluid (Fluid II) was formed mainly by the mixing of huge amount of magmatic fluid (very hot) with a minority of meteoric fluid, and also boiled. This fluid was also responsible for the potassic and then sericitic alteration zones in the lower and upper portion of the stock, respectively, and also remobilized Cu upwards. The third hydrothermal fluid (Fluid III) consisted of lower temperature, lower to moderate salinity (down to 5.7 wt % NaCl equiv.) oxidized meteoric water, which was responsible for peripheral propylitic alteration in a zone outside the core of potassically altered rock, and possibly argillic alteration when it was allowed to penetrate into the system. Final supergene enrichment of copper minerals was very limited, and consists of a thin blanket (up to 10

High temperatures phase changes

LV fluid inclusions homogenize to liquid ($Th_{L+V\rightarrow L}$) at temperatures between 523 ° and 298.1 °C in mineralized quartz veins. Almost all VL inclusions homogenize to vapor ($Th_{V+L\rightarrow V}$) between 351 ° and >600 °C, but some of the VL inclusions from population II quartz veins exhibit no changes until the temperature is within ~30 °C of the homogenization temperature; the vapor then rapidly expands to fill the inclusion, indicating a near-critical density fluid (cf. Roedder, 1984).

The liquid and vapor phases in $LVHS_1$ and $LVHS_2$ inclusions from population I homogenize to liquid at temperatures between ~351.0 ° and ~598.0 °C and between ~340 ° and ~578 °C in population II inclusions. The first mineral to dissolve in $LVHS_2$ inclusions is sylvite, at temperatures between 59.8 ° and 121.1 °C (Population I and II inclusions). Salinities based on the halite dissolution temperature range from 51.7 to 61.1 wt % NaCl equivalent (Sterner et al., 1988).

Most $LVHS_1$ and $LVHS_2$ inclusions in Population I and II veins homogenized by vapor disappearance. By contrast a few $LVHS_2$ inclusions homogenized mainly by halite dissolution. Anhydrite and chalcopyrite did not dissolve on heating to temperatures in excess of 600 °C.

Discussion

Pressure- temperature conditions

The maximum pressure of fluid entrapment can be calculated from the estimated thickness of the overlying rock column at the time of intrusion, which at Raigan is estimated to have been between 1.5 and 1.9 km. The latter represents ~500 m of Cretaceous limestone, plus 1100 to 1400 m of lower Tertiary volcanic, volcanoclastic, and related sedimentary rocks (based on the map and field observations). This corresponds to a lithostatic pressure of 400 to 500 bars (assuming an average rock density of 2.7 g/cm^3) and a hydrostatic pressure of 150 to 200 bars (assuming a fluid density near 1 g/cm^3).

Estimates of the temperatures of fluid entrapment can be made from the microthermometric and sulfur isotopic data (which is not measured in this case). In the case of LVHS inclusions the microthermometric data also permit independent estimates of pressure. As discussed earlier, the various fluid inclusion types are interpreted to represent three populations which, in principle, could have been trapped under different pressure-temperature conditions. $LVHS_1$ fluid inclusions occur with VL inclusions in population I quartz veins associated with potassic/phyllic alteration, and together with $LVHS_2$ fluid inclusions define fluid population I. The homogenization temperatures for type $LVHS_1$ inclusions (generally $Th_{L-V} > Tm_{Halite}$) vary between 538.8 ° and ~600 °C, and for co-existing VL inclusions vary between 455.4 ° and 600 °C; $LVHS_2$ inclusions homogenize at temperatures from 337.0 ° to 598.0 °C. At these temperatures the maximum pressure for the co-existence of these two fluid inclusion types (bubble point curve) is approximately 300 to 400 bars. On the other hand, the existence of LVHS fluid inclusions with $Tm_{Halite} > Th_{L-V}$ (mainly $LVHS_2$) implies that pressure was locally or temporarily much higher, assuming that the high values of Tm_{Halite} do not reflect accidental trapping or metastable dissolution of halite (cf. Chivas and Wilkins, 1977). If a single outlier is excluded, the pressures estimated for inclusions with $Tm_{Halite} > Th_{L-V}$ range as high as 800 bars, which exceeds the lithostatic pressure of 400 to 500 bars. We therefore propose that fluid pressure exceeded lithostatic pressure and that pressure generally oscillated between 150 to 200 bars (hydrostatic) and >500 bars in response to repeated cracking and sealing of the rock at a temperature of ~450 °C.

Fluid inclusion population III

LV fluid inclusions occur in all vein populations, but are most common in shallow quartz veins from phyllic and propylitic alteration zones (mainly in 21.90 to Rz-49 amples). They are clearly located along fracture planes, and are secondary in origin. LV inclusions appear to represent a later stage fluid that circulated in the intrusion.

Fluid inclusion microthermometry

Microthermometric studies were carried out on 17 samples of quartz from both veins and phynocrysts. Temperatures of phase changes in fluid inclusions were measured with a Fluid Inc. U.S.G.S.-type gas-flow (Linkam Operating System) stage which operates by passing preheated or precooled N_2 gas around the sample (Werre et al., 1979). Stage calibration was performed using synthetic and/or well-known fluid inclusions. Accuracy at the standard reference temperatures was ±0.2 °C at -56.6 °C (triple point of CO_2), ±0.1 °C at 0 °C (melting point of ice), ±2 °C at 374.1 °C (critical homogenization of H_2O), and ±9 °C at 573 °C (alpha to beta quartz transition). The heating rate was approximately 1 °C/min near the temperatures of phase transitions.

Low temperature phase changes

The temperatures of initial (T_e) and final melting of ice (Tm_{ice}) were measured on types LV, VL and LVHS fluid inclusions. In the case of type VL inclusions, T_e was difficult to determine, because of the high vapor/liquid ratios. Clathrate formation was not observed in any of the inclusions, which rules out the presence of significant CO_2. The crushing of quartz under anhydrous glycerine confirmed this conclusion; the vapor bubble collapsed during crushing in all but a few inclusions, and in the latter inclusions the bubble size was unchanged on increased slightly, indicating that the maximum pressure of incondensible gases was ~1 bar.

The temperature of initial ice melting (T_e) of most LV fluid inclusions was between -23 ° and –24.2 °C, suggesting that NaCl ± KCl are the principal salts in solution. The Tm_{ice} values for these inclusions range from –5.1 ° to –8.2 °C (Table 1), corresponding to salinities of 5.7 wt. % NaCl equiv., respectively (Sterner et al., 1988). A small proportion of very small (<2 μm) LV inclusions in quartz phenocrysts in shallow dykes have T_e between -25 ° and -39 °C, suggesting the presence of appreciable $CaCl_2$-$FeCl_2$- $MgCl_2$ in addition to NaCl and KCl, which I did not report it in the table 1 because of the size (Hezarkhani, 1997).

The T_e value of VL fluid inclusions ranges from –19.7 ° to –46.1 °C with a mode of ~-22 °C suggesting that Na and K are the dominant cations in the solution but that there are significant concentrations of divalent cations. The Tm_{ice} value for these inclusions varies from -0.4 ° to –12.1 °C, which corresponds to a salinity between 0.8 and 12.2 wt % NaCl equivalent.

Owing to the small volume of liquid in LVHS fluid inclusions, it is difficult to measure T_e and the melting temperature of hydro halite (Tm_{HH}). The eutectic temperatures that could be measured in population I and II inclusions ($LVHS_1$ and $LVHS_2$) range from –29.9 ° to -64.2 °C, suggesting important concentrations of Fe, Mg, Ca, and/or other components in addition to Na and K in this type of inclusion. Eutectic temperatures for the $CaCl_2$-H_2O, NaCl-$CaCl_2$-H_2O, and $FeCl_3$-H_2O systems are -49.8 °, -52 ° and -55 °C, respectively (Linke, 1965), and could explain the low first melting temperatures observed for some of the LVHS inclusions. Tm_{HH} values vary between –18.9 ° and –23.9 °C in LVHS inclusions. SEM-EDAX analyzes of the residues of decrepitated fluid inclusions is necessary to define the Fe and Ca in the inclusions.

Solid phases in fluid inclusions

Halite and sylvite in the inclusions were identified by their cubic and sub-cubic shapes and optical isotropy. The identification was confirmed by the both behavior and the shape. Sylvite was distinguished from halite by its rounded edges and lower relief; it also dissolves at lower temperatures. Halite crystals are generally larger and more common than those of sylvite, and have a well-defined habit. Chalcopyrite was identified on the basis of its optical characteristics (opacity and triangular cross section) and the composition could be proved by SEM-EDAX analyzes which may yielded peaks for Cu, Fe and S in opened inclusions. Anhydrite forms transparent anisotropic crystals. Hematite was easily identified from its red color, hexagonal shape, extremely high index of refraction and high birefringence (this identification also could be confirmed by SEM-EDAX analyzes on opened inclusions. A transparent, colorless to pale green solid with a rounded shape and strong birefringence, which dissolves at ~265 °C, could be the K-Fe chloride, erythrosiderite ($K_2FeCl_5. XH_2O$) (Hezarkhani A. and Williams-Jones, A. E. 1998).

Distribution of fluid inclusions types

VL inclusions are found in quartz phenocrysts and in quartz veins. Some of these inclusions occur in growth zones in quartz veins, where they are accompanied by LVHS fluid inclusions, indicating that at least some of them are primary. VL inclusions are generally elongate and have rounded ends, but some have negative crystal shapes. Some of the VL inclusions have variable liquid-vapor ratios, and may have formed from the necking-down of LVHS inclusions or heterogeneous entrapment of liquid and vapor.

LVHS inclusions up to 7 μm in diameter are found in all veins, from the deepest, potassically and phylically altered part of the stock through to the shallow level veins (based on the limited samples that I have). At shallow levels, most of the LVHS inclusions are of subtype S_2, but at deeper levels subtypes S_1 predominate. Up to seven solid phases have been observed in a single LVHS inclusion. The co-existence of LVHS inclusions (mainly $LVHS_2$) and vapor-rich inclusions with consistent phase ratios in the growth zones of quartz grains from potassic and phyllic alteration zones suggests a primary origin, and co-existence of two immiscible aqueous fluids.

Fluid inclusion population I

$LVHS_1$, $LVHS_2$ and VL fluid inclusions occur in quartz veins from the phylically altered zone (46 to 116 meters below the present erosional surface). In quartz veins, $LVHS_1$ and $LVHS_2$ fluid inclusions commonly form isolated clusters in the cores of quartz grains. VL inclusions commonly occur along microfractures, but they are also present in clusters with $LVHS_1$ fluid inclusions. $LVHS_1$, $LVHS_2$ and VL fluid inclusions that have been identified in quartz from veins in phyllic alteration zones at shallow levels may be relics of earlier potassic alteration. These three fluid inclusion types are interpreted to represent the earliest episode of fluid entrapment in the system.

Fluid inclusion population II

At shallower levels, in the phyllic alteration zone, there is a close spatial association of solid-rich $LVHS_1$ and VL fluid inclusions. They are found together in growth zones but occur mainly along healed fractures. This population of inclusions is spatially associated with LV inclusions, especially in both quartz veins and quartz phynocrystals, if, as discussed later, halite is a daughter mineral. The relative timing of entrapment of the two inclusion types is unclear.

Geological Setting of the Raigan Porphyry System

The Raigan porphyry system is hosted by a diorite/granodiorite to quartz-monzonite stock, located southeastern of Bam in the Kerman province of southeastern Iran (Fig. 1). The stock is located on the southeastern part of the Sahand-Bazman igneous and metallogenic belt (southeastern Iran), a deeply eroded Tertiary volcanic field, roughly 100 by 1700 km in extent (from Turkey to Baluchistan in southern Iran), consisting mainly of rhyolite and andesite, with numerous felsic intrusions. The volcanics were laid down unconformably over folded and eroded Upper Cretaceous andesitic volcanic and sedimentary rocks (~500 m thick). Subduction and subsequent continental collision during the Paleocene to Oligocene caused extensive alkaline and calc-alkaline volcanic and plutonic igneous activity, (including intrusion of a porphyritic calc-alkaline stock at Sungun and Sar-cheshmeh during the Miocene (Hezarkhani, 2003). Bordering the belt to the southwest is a major zone of complexly folded, faulted, and metamorphosed Tertiary and Paleozoic sedimentary rocks which form the Zagros Mountains (Waterman & Hamilton, 1975).

Fluid Inclusion Studies

Fluid inclusions in Raigan system are abundant in quartz of all vein types, and range in diameter from 1 μm up to 7 μm. The majority of inclusions examined during this study had diameters of 2-5 μm. They are also common in quartz phenocrysts (<3 μm). Most of the measurements were conducted on fluid inclusions in quartz from the rock matrix, with a few from mineralized quartz veins.

Fluid inclusion classification

Fluid inclusions were classified into three main types based on the number, nature, and proportion of phases at room temperature:

LV inclusions consist of liquid + vapor ± solid phases with the liquid phase volumetrically dominant. These fluid inclusions are common in all mineralized quartz veins and rock matrix. Their diameter range from 2 to 4 μm. Vapor bubbles are variable in size, but constitute less than 37 % of inclusion volumes. The inclusions homogenize to liquid. In a small number of LV fluid inclusions, a cube of halite (<1 μm in diameter), and unidentified transparent or opaque minerals (mainly hematite) were observed. The distribution and volume of solid phases are irregular, (< 3 % to > 11 %) suggesting that they represent trapped solids rather than daughter minerals.

VL inclusions also contain vapor + liquid ± solid phases. Vapor bubbles are variable in size, but in all cases consist of > 65 % of the inclusion volume. These inclusions mainly homogenize to vapour, and rarely to liquid, or by critical behaviour. Most VL inclusions contain only vapor + liquid. However, some inclusions contain a single solid phase which is either halite or an unidentified mineral, probably also trapped.

LVHS inclusions are multiphase, and consist of liquid + vapor + halite + other solids. Based on the number and type of the solids, we have further classified LVHS fluid inclusions into two subtypes. Subtype S_1 inclusions are characterized by the presence of halite + chalcopyrite ± anhydrite ± K-Fe-Cl ± sylvite phase (identification of this mineral is discussed below). Halite, anhydrite and chalcopyrite have consistent phase ratios and are interpreted to be daughter minerals. Vapour bubbles occupy < 20 % of the inclusion by volume. Subtype S_2 inclusions contain sylvite in addition to the phases in S_1 inclusions. The solid phases occupy ~60 % of inclusion volumes, and the vapour bubbles ~23 %.

are all associated with mid- to late-Miocene diorite/granodiorite to quartz-monzonite stocks. The Raigan porphyry system would be considered as a potential porphyry copper deposit, and it has been documented based on fluid-geochemical aspects.

The purpose of this paper is to elucidate the hydrothermal history of the Raigan porphyry system and identify the factors controlling Cu mineralization. To aid us in this task, the field observation, fluid inclusion microthermometry and phase relationships have have been documented.

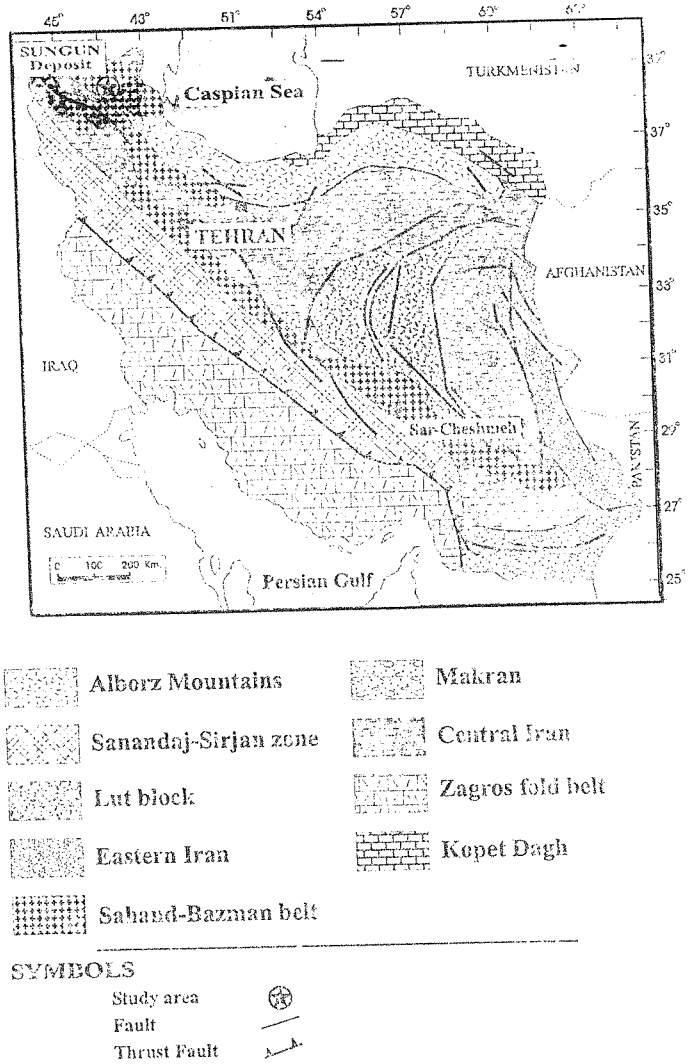

Figure (1) Geological map of Iran (modified from: Stöcklin, 1977; Shahabpour, 1994) showing major lithotectonic units as follows: *1) Zagros fold belt:* Paleozoic platform sediments overlain by miogeosynclinal Mid-Triassic to Miocene sediments, and syn-orogenic Pliocene-Pleistocene conglomerates; *2) Sanandaj-Sirjan zone:* Mesozoic granodioritic intrusions and metamorphosed Mesozoic sediments; *3) Central Iran zone:* Paleozoic platform sediments disrupted by late Triassic tectonic activity, and including horsts of Precambrian crystalline basement and Cambrian to Triassic cover rocks; *4) Sahand-Bazman belt:* Calc-alkaline volcanic and Quartz monzonite and quartz diorite intrusions of dominantly Miocene age, hosting Cu-Mo porphyry style mineralization; *5) Lut Block:* The Lut block is considered to be an old stable platform (Stöcklin, and Setudenia, 1972; Stöckline 1977), covered by thick Mesozoic sediments and Eocene volcanics; *6) Alborz and Kopeh Dagh zones:* Eocene volcanic and volcanoclastic rocks in the Alborz segment, and in the Kopeh-Dagh segment; *7) The Eastern Iran and Makran zones:* Post-Cretaceous flysch-mollasse sediments.

Hydrothermal Evolution in the Raigan Porphyry Copper System Based on Fluid Inclusion Studies, (Bam, Kerman, Iran): The Path to an Uneconomic Deposit.

A. Hezarkhani

Department of Mining, Metallurgical and Petroleum Engineering,
Amirkabir University of Technology

Abstract

The Raigan porphyry copper system is located in Bam, southeastern Iran (Kerman province), and is associated with diorite/granodiorite to quartz-monzonite of Miocene age that intruded Eocene volcano-sedimentary rocks. Copper mineralization was accompanied by mainly phyllic and less potassic alteration. Field observations and petrographic studies demonstrate that emplacement of the Raigan stock took place in several intrusive pulses, each with associated hydrothermal activity. Molybdenum is not reported in any stage of hydrothermal evolution through the system. Due to lack of information, the petrogenesis interpretation is mainly based on the field observation. It seems that early hydrothermal alteration produced a potassic assemblage (orthoclase-biotite) in the central part of the stock, propylitic alteration occurred contemporaneously with potassic alteration, but in the peripheral parts of the stock, and phyllic alteration formed later, overprinting all the earlier alteration (the most majority alteration in the Raigan system). The early hydrothermal fluids are represented by high temperature (487 °C to 598 °C), high salinity (up to 61.1 wt % NaCl equiv.) liquid-rich fluid inclusions, and high temperature (397 °C to 401 °C), low-salinity, vapor-rich inclusions. These fluids are interpreted to represent an orthomagmatic fluid which boiled episodically; the brines are interpreted to have caused potassic alteration, containing first generation of chalcopyrite. Propylitic alteration is attributed to a liquid-rich, lower temperature (523 °C to 298 °C), Ca-rich, evolved meteoric fluid. Influx of meteoric water into the system, and mixing with magmatic fluid produced deep albitization, and shallow phyllic alteration. This influx also caused dissolution of early formed copper sulfides and remobilization of Cu into the sericitic zone where it was resystemed in response to a boiling-induced decrease in temperature. Supergene alteration was minor and restricted to a thin blanket of Cu-sulfides.

Key words

Hydrothermal, Raigan Bam, Copper, Iran

Introduction

In Iran, all known porphyry copper mineralization occurs in the Cenozoic Sahand-Bazman orogenic belt (Fig. 1). This belt was formed by subduction of the Arabian plate beneath central Iran during the Alpine orogeny (Hezarkhani, 2002; Berberian, and King, 1981; Pourhosseini, 1981; Niazi, and Asoudeh, 1978) and hosts two major porphyry Cu deposits. The Sar-Cheshmeh deposit is the only one of these being mined, and contains 450 million tonnes of sulfide ore with an average grade of 1.13 % Cu and ~0.03 % Mo (Waterman and Hamilton, 1975). The Sungun deposit, which contains >500 million tonnes of sulfide reserves grading 0.76 % Cu and ~0.01 % Mo, is currently being developed. Sar-Cheshmeh, Sungun and a number of subeconomic porphyry copper deposits